Insulin Unmasks a COOH-Terminal Glut4 Epitope and Increases Glucose Transport across T-Tubules in Skeletal Muscle

Weichen Wang,* Polly A. Hansen,‡ Bess A. Marshall,* John O. Holloszy,‡ and Mike Mueckler*

*Department of Cell Biology and Physiology and ‡Department of Medicine, Washington University School of Medicine, St. Louis, Missouri 63110

Abstract. An improved immunogold labeling procedure was used to examine the subcellular distribution of glucose transporters in Lowricryl HM20–embedded skeletal muscle from transgenic mice overexpressing either Glut1 or Glut4. In basal muscle, Glut4 was highly enriched in membranes of the transverse tubules and the terminal cisternae of the triadic junctions. Less than 10% of total muscle Glut4 was present in the vicinity of the sarcolemmal membrane. Insulin treatment increased the number of gold particles associated with the transverse tubules and the sarcolemma by threefold. However, insulin also increased the total Glut4 immunogold reactivity in muscle ultrathin sections by up to 1.8-fold and dramatically increased the amount of Glut4 in muscle sections as observed by laser confocal immunofluorescence microscopy. The average diameter of transverse tubules observed in longitudinal sections increased by 50% after insulin treatment. Glut1 was highly enriched in the sarcolemma, both in the basal state and after insulin treatment. Disruption of transverse tubule morphology by in vitro glycerol shock completely abolished insulin-stimulated glucose transport in isolated rat epitrochlearis muscles. These data indicate that: (*a*) Glut1 and Glut4 are targeted to distinct plasma membrane domains in skeletal muscle; (*b*) Glut1 contributes to basal transport at the sarcolemma and the bulk of insulin-stimulated transport is mediated by Glut4 localized in the transverse tubules; (*c*) insulin increases the apparent surface area of transverse tubules in skeletal muscle; and (*d*) insulin causes the unmasking of a COOH-terminal antigenic epitope in skeletal muscle in much the same fashion as it does in rat adipocytes.

GLUCOSE transport in the insulin-sensitive tissues has received considerable experimental attention because of the importance of this process in the maintenance of whole-body glucose homeostasis (38). Transport into skeletal muscle is of particular physiological importance because this tissue represents the major site of glucose disposal in the postprandial state (17), and defects in glucose uptake into muscle contribute to the pathogenesis of type II diabetes mellitus (5, 46). The influx of glucose into skeletal muscle appears to be mediated by two glucose transporter isoforms, Glut1 (4, 39) and Glut4 (3, 7, 19, 29). Glut4 is at least 10-fold more abundant in muscle cells than is Glut1, and it is this isoform that is responsible for the acute increase in glucose uptake observed in response to elevated insulin or contractile activity (24, 50). A distinct role for muscle Glut1 has not been clearly defined, although transgenic overexpression studies suggest that Glut1 mediates basal glucose transport into skeletal muscle fibers (21, 36, 44). Insulin rapidly stimulates glucose uptake into muscle by a mechanism that may involve the subcellular redistribution of Glut4 from intracellular membrane compartments to plasma membrane domains (33, 45, 53).

The current concept that Glut4 translocates from intracellular compartments to the plasma membrane in response to insulin is strongly supported by observations in adipocytes, where translocation has been clearly demonstrated using a combination of methodologies, including subcellular fractionation (9, 55), photoaffinity labeling (26), and quantitative ultrastructural examination using immunogold labeling (48). However, the process may be more complicated than is currently appreciated. For example, an immunogold labeling study suggests that conformational changes involving the unmasking of an antigenic epitope may contribute to insulin-stimulated transport activity in primary cultures of rat adipocytes (49).

The mechanism of glucose transporter regulation in skeletal muscle is more obscure than in adipocytes because of the technical difficulties involved in performing cell biological experiments on this tissue. Skeletal muscle

Address all correspondence to Mike Mueckler, Department of Cell Biology and Physiology, 660 S. Euclid Ave., St. Louis, MO 63110. Tel.: (314) 362-4160. Fax: (314) 362-7463. E-mail: mike@cellbio.wustl.edu

fibers have a distinct architecture compared to adipocytes and contain two different plasma membrane domains, the sarcolemma and T-tubules. The precise subcellular distribution of Glut1 and Glut4 in skeletal muscle and the location of basal- and insulin-stimulated transport into the muscle fiber are fundamental issues that remain unresolved. Depending on the technique used, ultrastructural studies have indicated that in unstimulated muscle fibers, Glut4 is enriched in subsarcolemmal vesicles (45), triadic junctions (12, 18), or both of these structures (6). Translocation to the sarcolemma has been reported in at least two of these studies. However, in none of these studies was quantification of the Glut4 distribution attempted. The ultrastructural investigation of the distribution of Glut1 in muscle has not yet been explored because of the very low abundance of this protein in normal muscle. Subcellular fractionation studies have also produced somewhat contradictory results. Redistribution of Glut4 to subcellular fractions enriched in markers for the sarcolemma (11, 25) and the T-tubules (32, 40) has been reported, but it is unclear which of these domains is most important in insulin-stimulated transport.

We have addressed these unresolved questions by implementing an improved immunogold labeling procedure for plastic-embedded thin sections and by using a hypertonic shock technique to examine the effect of T-tubule disruption on glucose transport. Additionally, we used transgenic mice overexpressing either Glut1 or Glut4 in skeletal muscle to enhance the immunolabeling density and to enable accurate quantification of the ultrastructural data. Our data indicate that Glut1 and Glut4 are targeted to different plasma membrane domains in skeletal muscle. Furthermore, our results suggest that basal transport occurs via Glut1 localized constitutively at the sarcolemma, and that insulin-stimulated transport occurs primarily via Glut4 located at the T-tubule. Our data also suggest that insulin induces conformational changes in skeletal muscle Glut4 similar to its effect in the adipocyte.

Materials and Methods

Materials

Insulin (HumulinR) was purchased from Eli Lilly and Co. (Indianapolis, IN). 3-*O*-[^{3}H]Methyl-D-glucose and [^{14}C]mannitol were purchased from Dupont/NEN Research Products (Boston, MA). Lowricryl HM20 and Epon 812 embedding media were purchased from Polysciences, Inc. (Warrington, PA). The primary antibodies used were: a rabbit polyclonal antiserum (F349) raised against a synthetic peptide corresponding to the COOH-terminal 16 residues of rat Glut4, a rabbit polyclonal antiserum (F350) raised against a synthetic peptide corresponding to the COOH-terminal 16 residues of human Glut1 (23), and a rabbit polyclonal antiserum (WU626) raised against a synthetic peptide corresponding to residues 245–266 of rat Glut4. The antibodies were purified using corresponding immunoaffinity columns (43). The peptides against which these antibodies were raised were coupled to Thiopropal Sepharose 6B (Sigma Chemical Co., St. Louis, MO). The specificity of the purified F349 and F350 antibodies has been verified extensively (22, 23, 27, 28, 35). Goat anti–rabbit IgG colloidal gold conjugate was purchased from Jackson ImmunoResearch Laboratory, Inc. (West Grove, PA).

The Transgenic Mice

The construction of transgenic mice carrying a human Glut4 (hGlut4) glucose transporter minigene construct (42) or carrying a human Glut1 glucose transporter minigene construct (36) has been described previously. The pattern of tissue-specific expression of the Glut4 construct has been shown to follow that of the endogenous mouse Glut4 gene (42). Heterozygous hGlut4-11.5B transgenic mice (31) and their nontransgenic littermates (8–13-wk old) were used in all experiments. The Glut1 minigene in the Glut1 construct contains a 2.47-kb cDNA fragment encoding the human Glut1 glucose transporter under the regulation of the 1.2-kb rat myosin light chain-2 promoter. Expression of the transgene is restricted to skeletal muscle and dose not affect expression of the endogenous Glut4 isoform (36). Animals were housed in a room maintained at 23°C with a fixed 12 h light–dark cycle and given access to Purina Chow and water ad libitum.

Immunoelectron Microscopy

Muscles were subjected to insulin stimulation using three different protocols. (1) Mice were given glucose (2 g/kg body weight) and 6 U of insulin intraperitoneally 30 min before in situ fixation. Control mice were injected with vehicle alone. The injected mice were anesthetized with 80 mg/kg sodium pentobarbital and perfusion fixed via intracardiac puncture with 3% paraformaldehyde and 0.5% glutaraldehyde in PBS (0.14 M NaCl, 2.7 mM KCl, 1 mM $CaCl_2$, 1.5 mM KH_2PO_4, 8.1 mM Na_2HPO_4, pH 7.4). The quadriceps or soleus muscles were dissected and further fixed for 2 h in the same solution. (2) Mice were subjected to a euglycemic, hyperinsulinemic clamp as described under "Hyperinsulinemic Clamp." The left soleus muscle was removed at the end of the basal clamp period and the right soleus muscle was removed at the end of the insulin infusion period. The muscles were then fixed in 3% paraformaldehyde, 0.5% glutaraldehyde as described above. (3) Epitrochlearis muscles were removed from anesthetized mice and incubated in vitro in the presence or absence of insulin as described under "In Vitro Muscle Incubation and Selective Disruption of T-Tubules." The muscles were then fixed in 3% paraformaldehyde, 0.5% glutaraldehyde as described above.

After fixation, the tissues were rinsed with PBS and distilled water and in bloc stained with 0.5% uranyl acetate for 30 min at 4°C. The tissues were dehydrated through graded ethanol: 30% for 10 min at 4°C, 50% for 1 h at −20°C, 70% for 1 h, 95% for 1 h, and 100% for 2 h with three changes all at −45°C. The tissues were embedded in Lowricryl HM20 and polymerized under 360-nm UV light for 1 d at −45°C, 1 d at −35°C, and 1 d at room temperature under sun light.

The cut thin sections were picked on nickel grids coated with Polyvinyl formal film. The nonspecific binding sites were blocked by incubating sections with 5% goat serum for 15 min and 2% gelatin for 10 min. The sections were washed with PBS and then incubated with primary antibody for 1 h at 37°C, followed by six washes in PBS and then incubation with goat anti–rabbit IgG colloidal gold conjugate for 30 min at room temperature. To determine levels of nonspecific labeling, preimmune IgG was substituted for the primary antibody, or the primary antibody was saturated with a 10-fold molar excess of the peptide used to raise the antibody. The grids were then stained with 4% uranyl acetate for 20 min and Reynold's lead solution for 50 s and examined in an electron microscope (model 902; Carl Zeiss, Inc., Thornwood, NY).

For quantification of the immunogold labeling, measurements of T-tubule dimensions were made from the electron micrographs using a 7× eyepiece magnifier with a graticule divided at 0.1-mm intervals (Ted Pella, Inc., Redding, CA). Immunogold labeling density was determined in micrographs of longitudinal sections, with each sarcomere defined as the basic quantification unit. Quantification of labeling in the region of the sarcolemma was based on the number of gold particles observed per 2 μm length. All quantification data presented here were repeated at least twice in independent experiments. The nonspecific background labeling determined using either preimmune IgG or by competition with excess immune peptide was extremely low under the optimal conditions described above (<1% of the specific labeling for either Glut1 or Glut4 labeling).

Isolation of Intact Triads

Total skeletal muscles from seven Glut4 transgenic mice were pooled and homogenized in 10% sucrose, 0.5 mM EDTA, pH 7.2. The homogenate was centrifuged at 9,000 rpm for 15 min in a rotor (model JA-10; Beckman Instrs., Fullerton, CA) and the supernatant was filtered through cheesecloth and recentrifuged at 30,100 *g* for 30 min to produce the heavy microsome fraction. The pellet was homogenized again with a Dounce homogenizer and loaded on top of a sucrose gradient composed of a 28–50% continuous sucrose gradient and 25, 14, and 10% step gradients. Centrifugation was carried out using a rotor (model SW 28.1; Beckman Instrs.) at

97,000 *g* at 4°C for 90 min (37). The band enriched in triads was collected, fixed, and processed for immunoelectromicroscopy as described above.

Hyperinsulinemic Clamp

Clamp experiments were carried out as previously described (34) with the following modifications: After placement of the infusion catheter, an infusion of 3-[^{3}H]glucose at 0.04 μCi/min was begun for measurement of the rate of appearance of glucose, hepatic glucose production, and total body glucose utilization. The infusion was continued during a 1-h control period, and 20 μl of blood was taken from the tail for determination of glucose specific activity at 45 and 60 min. After 60 min, an infusion of insulin 20 mU/kg/min was begun and continued for at least 90 min. Dextrose infusion (25%) was begun and the infusion rate was varied to maintain the blood glucose at the level it appeared during the last 15 min of the control period. The continuous infusion of 3-[^{3}H]glucose tracer was continued during the insulin infusion period and, in addition, tracer was added to the 25% dextrose infusion to approximate the glucose-specific activity in the blood at the end of the control period. This approximation was based upon measurement of specific activity during identical conditions in the same type of mice in previous experiments. Blood samples for determination of specific activity were taken 15 min before and at the end of the insulin infusion period, when the blood glucose was in a steady state. The combined gastrocnemius/soleus/plantaris muscles were excised during the clamp experiment, the right muscles at the end of the control period and the left muscles at the end of the insulin infusion period. One-half of each muscle sample was rapidly frozen in liquid nitrogen and used for Western blot analysis, and the other half was immersed immediately in fixative and used for confocal immunofluorescence microscopy.

Specific activity was determined by aqueous scintillation counting of 20 μl of blood deproteinized with 5 ml each of barium hydroxide (0.3 N) and zinc sulfate (0.3 N). The supernatant resulting from the deproteinization was dried at 70°C to remove tritiated water before resuspension and counting.

The rate of appearance of glucose (R_a), which equals the rate of total body glucose utilization when the blood glucose is in steady state, was calculated by dividing the infusion rate of 3-[^{3}H]glucose by the specific activity of glucose at the same time. Hepatic glucose production (HGP) was calculated by subtracting the cold glucose infusion rate from R_a.

Western Blot Analysis and Confocal Immunofluorescence Microscopy

Combined soleus/gastrocnemius/plantaris muscles were removed from the hind limbs of mice before and after a hyperinsulinemic/euglycemic clamp as described above. One-half of each muscle sample was processed for laser confocal immunofluorescence microscopy, and the other half was subjected to Western blot analysis as previously described (36) using a rabbit polyclonal IgG antibody directed against the COOH terminus of Glut4 (F349). The Glut4 protein standard was prepared by expression of rat Glut4 in *Xenopus* oocytes as previously described (35).

The muscle samples were prepared for immunofluorescence microscopy by fixation in 4% paraformaldehyde and 0.4% glutaraldehyde in 0.1 M cacodylate buffer, pH 7.4, for 2 h, rinsed three times with the same buffer over a 30-min period, incubated in a solution containing 30% sucrose, 20% polyvinylpyrollidone, 44 mM sodium carbonate, and 20 mM phosphate buffer, pH 7.4, at 4°C overnight, and then frozen. 15-μm cryosections were cut and mounted on glass slides. The sections were rinsed at room temperature in PBS and then incubated in 0.1% Triton-X 100 at room temperature for 10 min, 2.5% normal goat serum for 15 min, 2% gelatin for 15 min, followed by a rinse in PBS before incubation with primary antibody at 37°C for 1 h. Slides were then rinsed with PBS and incubated in fluorescein-conjugated goat F(ab')2 anti-rabbit IgG (Chemicon International, Inc., Temecula, CA) at room temperature for 45 min. The primary antibody for detection of Glut4 was an IgG fraction of F349 Glut4 antiserum prepared using protein A–Sepharose (Sigma Chemical Co., St. Louis, MO). Nonspecific labeling was assessed using preimmune IgG. Under the conditions used for the micrographs presented in this paper, all of the observed fluorescence represents specific labeling, i.e., fields from control slides appeared completely black.

In Vitro Muscle Incubation and Selective Disruption of T-Tubules

Male Wistar rats (80–110 g) obtained from SASCO (Omaha, NE) were used for the T-tubule disruption experiments. Rats were used rather than mice because their muscles are more insulin sensitive. Rats were anaesthetized by an intraperitoneal injection of pentobarbital sodium (5 mg/100 g body weight) and the epitrochlearis or soleus muscles were removed (54). Immediately after dissection, muscles were initially incubated at room temperature for 60 min in 2 ml of Ringer's buffer (115 mM NaCl, 2.5 mM KCl, 1.8 mM $CaCl_2$, 3.0 mM phosphate buffer, pH 7.0), in the presence or absence of 400 mM glycerol (13), and then transferred to 2 ml glycerol-free Ringer's for 30 min. Muscles were then incubated for 20 min at 35°C in 2 ml of oxygenated Krebs-Henseleit buffer (KHB) supplemented with 2 mM sodium pyruvate, 36 mM mannitol, and 0.1% radioimmunoassay grade BSA, in the presence or absence of 10 mU/ml insulin before measurement of glucose transport activity. All incubations were performed in a Dubnoff shaking incubator (Precision Scientific, Chicago, IL). Flasks were gassed continuously with 95% O_2, 5% CO_2 throughout the experiment. For T-tubule recovery experiments, the muscle samples were returned to glycerol-containing Ringer's solution for 40 min before proceeding to the next step. The muscles were then either processed for electron microscopy or for glucose transport measurements.

Measurement of Glucose Transport Activity

Glucose transport activity was measured using previously described methods (54). After the initial incubations, muscles were transferred to 1.0 ml KHB containing 8 mM 3-*O*-[^{3}H] methyl-D-glucose (294 μCi/mmol), 32 mM [U-^{14}C]mannitol (8 μCi/mmol), 0.1% BSA, and the same concentration of insulin present during the previous incubation. The temperature was maintained at 35°C and the flasks were gassed continuously with 95% O_2, 5% CO_2. To terminate the transport assay, muscles were blotted at 4°C and clamp frozen. Extracellular space and intracellular 3-*O*-methylglucose concentration (μmol·ml intracellular water $^{-1}$·10 min^{-1}) were determined as previously described (54).

Results

Two technical problems have often been encountered by researchers using Lowricryl HM20 as an embedding medium for immunogold labeling studies. The first is low contrast of membranous structures within the cell, which makes accurate quantification of immunogold-labeled membrane proteins difficult if not impossible. The second is low antibody labeling efficiency compared with that obtained using standard frozen sections. We made two simple but effective modifications to the general procedure that eliminated these two problems. The use of a low concentration of uranyl acetate (0.5%) for a short period of in bloc staining before embedding the tissue was used to increase the contrast of membrane structures and to greatly enhance the general morphology of the thin section, without interfering with tissue polymerization (overly stained tissue would inhibit UV light penetration) or antibody labeling. Additionally, the time and temperature of the primary antibody incubation was found to be critical for obtaining good labeling efficiency with low background staining. Incubating Lowricryl HM20–embedded tissue sections at 37°C for 1 h rather than prolonged incubation at either room temperature or 4°C greatly increased the specific labeling efficiency and dramatically decreased nonspecific binding. The signal to noise ratio obtained with the optimized labeling procedure was >100:1, i.e., the number of gold particles observed in muscle sections when preimmune IgG was substituted for immune IgG or when an excess of immune peptide was used to compete out specific binding sites was <1% of specific labeling.

This technique was used to localize glucose transporter isoforms in the skeletal muscle of transgenic mice overexpressing either Glut1 or Glut4. Glut1 was primarily located on the sarcolemma in Glut1 transgenic mice (Fig. 1).

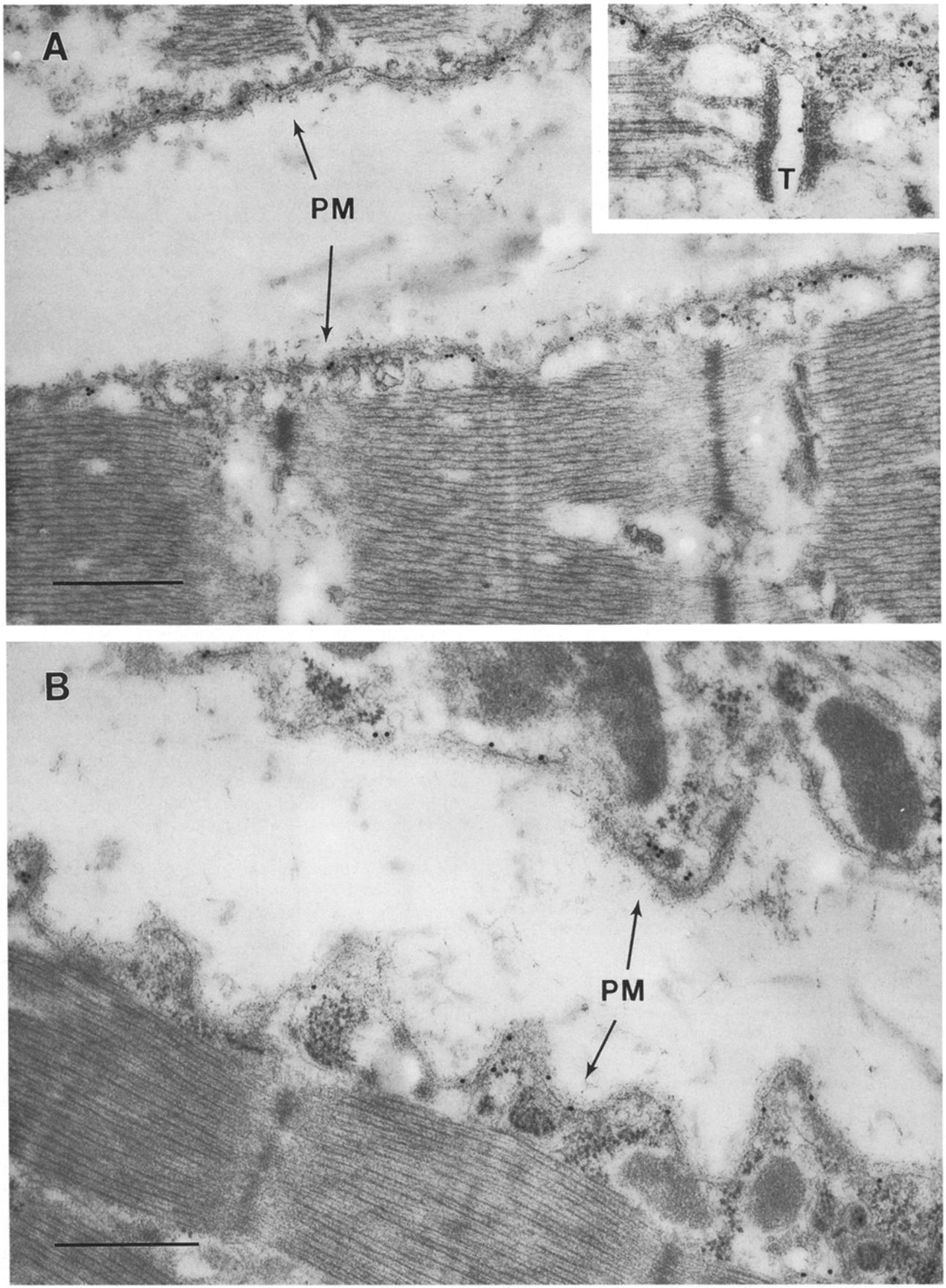
A
PM
T
B
PM

Table I. Subcellular Distribution of Glut4 in Skeletal Muscles of Glut4 Transgenic Mice

Group	No. animals used	Condition	Gold particle count: Sarcolemma (per 2 μm length) PM	Sarcolemma (per 2 μm length) Space under PM	Sarcomere (1 × 2 μm) Total	Sarcomere (1 × 2 μm) Triad	Sarcomere (1 × 2 μm) T-tubules
Insulin clamp–infusion	3	Basal	3 ± 0.3	7 ± 1.0	28 ± 3.1	19 ± 2.8	8 ± 2.2
		Insulin	8 ± 2.1	4 ± 0.2	46 ± 4.3	26 ± 3.7	16 ± 3.7
In vitro muscle incubation	3	Basal	7 ± 1.2	8 ± 1.5	19 ± 2.1	17 ± 1.7	8 ± 0.5
		Insulin	9 ± 1.7	7 ± 0.8	25 ± 2.7	20 ± 2.1	12 ± 0.9
In vivo peritoneal administration	6	Basal	9 ± 0.7	14 ± 1.1	34 ± 2.4	26 ± 1.7	12 ± 1.1
		Insulin	14 ± 0.6	9 ± 0.4	60 ± 3.7	43 ± 3.7	26 ± 1.2

Three experimental procedures were used to examine the effect of insulin on the distribution of Glut4 in skeletal muscles. (1) Insulinemic clamp–infusion. The right soleus muscle was removed from an anesthetized Glut4 transgenic mouse at the end of the basal clamp period and the left soleus muscle was removed at the end of the hyperinsulinemic clamp period. The muscle samples were then fixed, embedded in Lowricryl HM20, and processed for immunoelectron microscopy as described in Materials and Methods. (2) In vitro muscle incubation. Pairs of epitrochlearis muscles were removed from Glut4 transgenic mice and incubated in either the absence or presence of insulin for 30 min as described in Materials and Methods. The muscles were then processed for immunoelectron microscopy. (3) In vivo peritoneal administration. Either insulin and dextrose or buffer alone (for basal mice) was injected i.p. into Glut4 transgenic mice 30 min before in situ fixation of muscles. Hindlimb quadriceps muscles were then removed and processed as described in Materials and Methods. Each of the protocols was conducted on muscles obtained from the total number of animals indicated, and in each case, 2–3 independent experiments were performed. The numbers represent the mean ± SE. The Student's *t*-test was used to determine the significance of the differences between basal and insulin treatment for each experiment. For quantification of total intracellular Glut4 (apart from Glut4 beneath the sarcolemma), gold particles were counted in longitudinal sections encompassing 1 × 2 μm (roughly equivalent to the size of a sarcomere) and containing two T-tubule profiles. Between 30–50 total sarcomeric units were quantitated per experiment. For quantification of Glut4 on T-tubule membranes, the number of gold particles were counted per 1 μm length of membrane. Note that gold particles appear on both cytoplasmic faces of each T-tubule membrane observed in longitudinal section. For quantification of Glut4 on the sarcolemma, the number of gold particles are expressed per 2 μm length of membrane. Between 100–120 μm of sarcolemma was quantitated per experiment. For quantification of Glut4 in vesicles beneath the sarcolemma, gold particles are expressed per 2 μm length of sarcolemma and extending in depth down to the first myofibril. Gold particles within ~15 nm of a bilayer structure were considered to be in the membrane. *PM*, plasma membrane.

It was also detected on T-tubule membranes but at a much lower abundance (Fig. 1 *A*, *Inset*). The level of Glut1 in the wild-type mouse was so low that it could not be detected by this method. Short-term insulin treatment did not change the Glut1 labeling density on the sarcolemmal membrane or the T-tubular membrane. The insulin-treated group had an average of 6.6 ± 0.57 particles per 2.2 μm on the sarcolemma (2.2 μm is equivalent to the average length of a sarcomere) and 1.1 ± 0.22 on T-tubules, compared to 6.2 ± 0.95 particles on the sarcolemma and 1.3 ± 0.23 on T-tubules for the basal group. Statistically, there was no significant difference between the insulin-treated and control groups. Intracellular Glut1 labeling in either condition was very low (Fig. 1, *A* and *B*).

Glut4 could be readily detected in muscle ultrathin sections from both wild-type and transgenic mice. The quantitative results presented here are for the Glut4 transgenic mice. Very similar results were observed for the wild-type mice, although the labeling density was reduced. Three different protocols were used to examine the subcellular distribution of Glut4 in basal and insulin-treated muscle: (1) intraperitoneal injection of mice with insulin followed by in situ perfusion fixation; (2) isolation of individual muscles from untreated animals followed by in vitro incubation with or without insulin; and (3) removal of muscles from mice before or after a 90-min euglycemic/hyperinsulinemic clamp followed by in vitro fixation. The results obtained with the different protocols were quantitatively different but were in good qualitative agreement (Table I).

The great preponderance of Glut4 labeling under basal and insulin-treated conditions was located in and around the muscle triad (Fig. 2). Heavy labeling was observed both in T-tubule membranes and in the closely associated terminal cisternae. A lesser amount of labeling was also observed in the regions of the sarcoplasmic reticulum membranes. The possibility that the latter labeling was in some undefined structures closely associated with either the terminal cisternae or sarcoplasmic reticulum cannot be excluded by these methods. However, the labeling observed in this region was of a specific nature, because it was not observed under control conditions. To examine the Glut4 labeling of the triad region further, triad structures were isolated from muscle homogenates by subcellular fractionation and then subjected to immunogold labeling. Gold particles were again observed in both T-tubular membranes and in the closely associated lobules representing the terminal cisternae (Fig. 3).

Glut4 labeling in basal and insulin-treated muscle was also observed in the sarcolemma and more frequently in vesicles beneath the sarcolemma (Fig. 2, *A* and *B*). As was reported previously, some Glut4 in this region was present in vesicles in close proximity to Golgi stacks (data not shown). However, Golgi stacks were only observed in the vicinity of nuclei and were relatively sparse. Glut4 in these regions represented <1% of the total muscle labeling. We estimate that >90% of total muscle Glut4 was located in the region of the triadic junctions and that <10% of total Glut4 was located in the vicinity of the sarcolemma (see Discussion).

Insulin increased the number of gold particles that were

Figure 1. Ultrastructural localization of Glut1 in Lowricryl HM20–embedded Glut1 transgenic mouse muscles. The thin sections were stained with an antibody specific for the COOH terminus of Glut1 (F350) and a colloidal gold conjugated secondary antibody. Glut1 was primarily located on the sarcolemma. Short term insulin treatment (up to 30 min) did not change the distribution pattern of Glut1 in skeletal muscle (*A*, basal; *B*, insulin). Glut1 was also detected on T-tubules but with much less abundance (*Inset*). *PM*, plasma membrane; *T*, T-tubule. Bar, 0.5 μm.

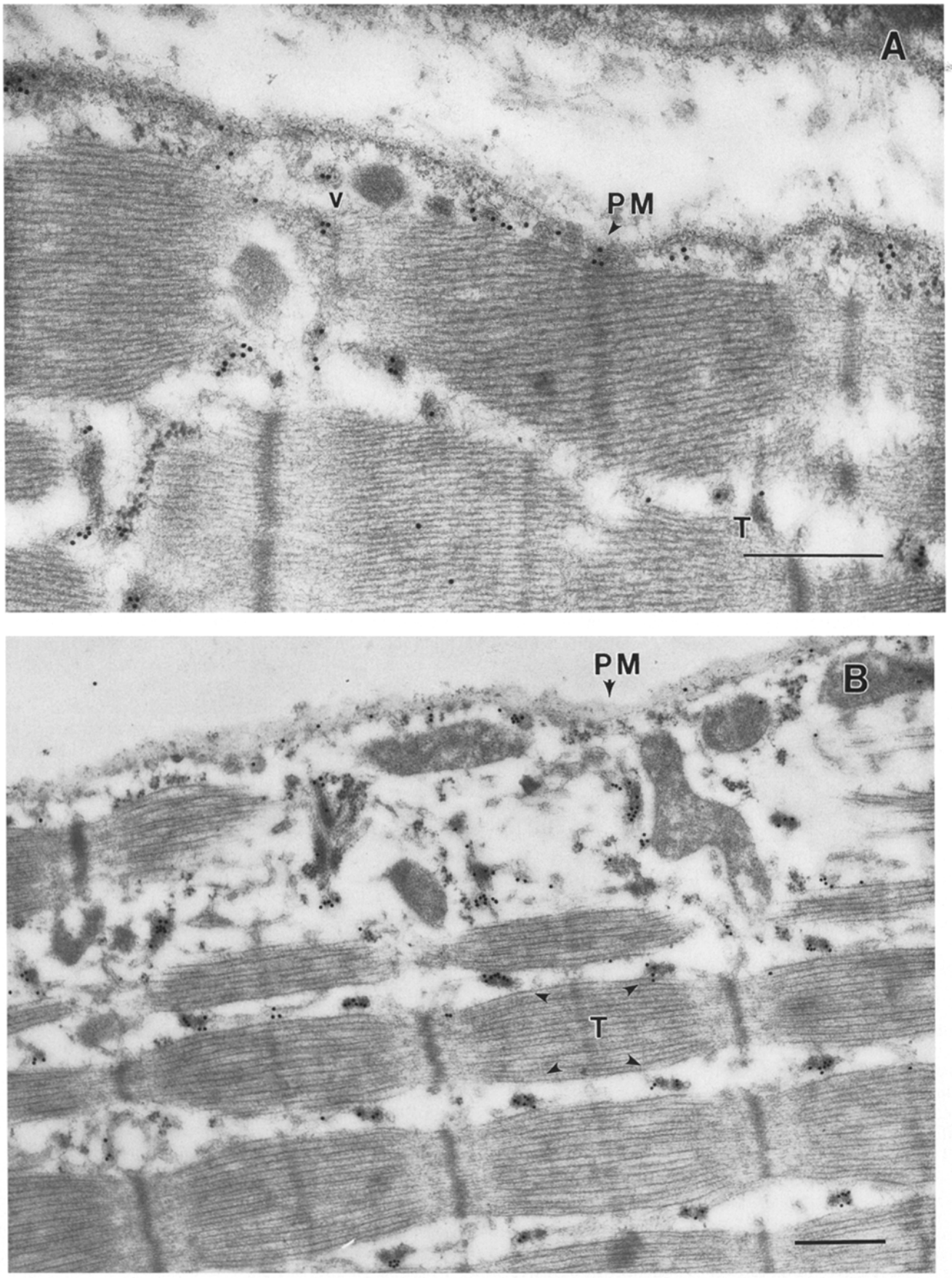
A
V
PM
T
PM
B
T

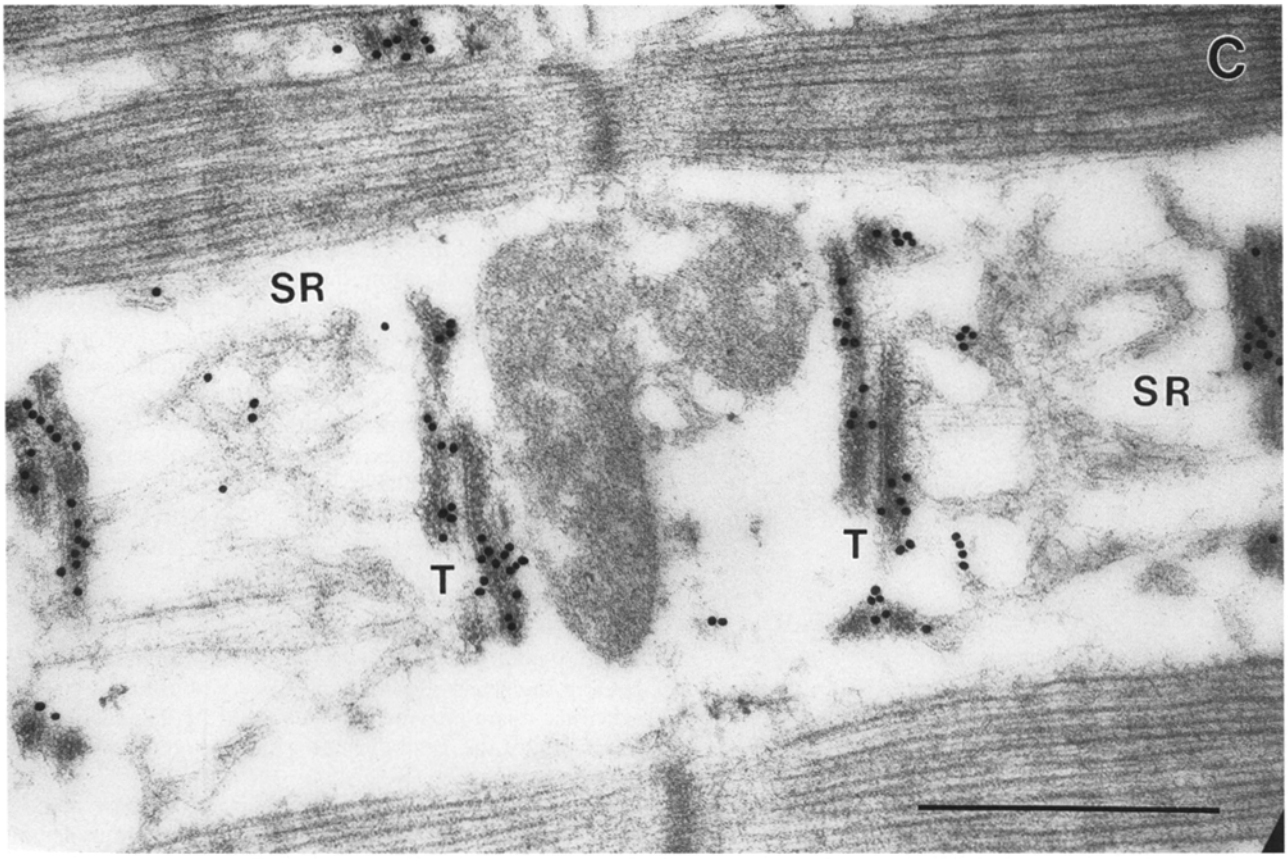

Figure 2. Ultrastructural localization of Glut4 in Lowricryl HM20–embedded Glut4 transgenic mouse muscles. The thin sections were stained with an antibody specific for the COOH terminus of Glut4 (F349) and a colloidal gold–conjugated secondary antibody. Both the sarcolemma and T-tubules were labeled with anti-Glut 4 antibody. (*A*) In the basal state, most of the gold particles in the vicinity of the sarcolemma were actually in vesicles beneath the surface membrane. (*B*) This micrograph shows the general labeling pattern of Glut4 transgenic mouse muscles in the insulin stimulated state. More than 90% of the gold particles were located at the A-I junction, mostly on T-tubule membranes and around the triad. Notice that the sarcolemmal membrane was also more heavily labeled than in the basal state. Insulin increased Glut4 labeling on the sarcolemma by about threefold. (*C*) High magnification micrograph showing Glut4 labeling along the T-tubular membrane. Insulin increased Glut4 labeling on the T-tubular membrane by ~twofold. *PM*, Plasma membrane; *SR*, Sarcoplasmic reticulum; *T*, T-tubule; *v*, Glut4-containing vesicle. Bar, 0.5 μm.

associated with T-tubules by up to twofold and increased gold particles in the sarcolemma by up to threefold (Table I). However, insulin treatment also caused an increase in the total number of gold particles observed in the muscle sections. This increase in total labeling was observed with all three insulin-treatment protocols (Table I). For example, the i.p. administration of insulin resulted in an increase in total particles per sarcomere from 34 to 60 ($P < 0.001$). The increase in immunoreactive Glut4 in muscle sections was verified by laser confocal immunofluorescence microscopy using the same Glut4 antibody raised against the COOH terminus of the protein as was used for the immunogold labeling (Fig. 4, *a* and *b*).

We next performed immunoblots on total muscle homogenates to determine whether the short-term insulin treatment resulted in an increase in total muscle Glut4 protein. The immunoblot data indicate that insulin did not increase the total Glut4 content of the skeletal muscle (Fig. 5 *B*). One possible explanation for these data is that the COOH-terminal epitope of Glut4 recognized by the antibody is partially masked in the basal state, and that insulin unmasks the epitope and thereby increases the labeling efficiency of Glut4. These data are thus reminiscent of the epitope unmasking previously reported for Glut4 labeling of the adipocyte plasma membrane after insulin treatment (49). Although the semiquantitative ultrastructural data presented in Table I appear to indicate that there were equivalent increases in immunoreactive Glut4 in the T-tubule membranes and the surrounding intracellular membrane systems, it should be pointed out that it can be extremely difficult to determine whether a gold particle is actually in the T-tubule membrane or in the very closely associated terminal cisternae (or some other undefined membrane structures in this region). Thus, it is quite possible that a disproportional increase in T-tubule Glut4 labeling occurred but could not be detected by our methods.

Smith et al. used an antibody directed against the NH_2 terminus of Glut4 to demonstrate that the insulin-induced antigenic unmasking of the COOH terminus observed in adipocytes is specific in the sense that it does not extend to the NH_2 terminus. We tested the specificity of the antigenic unmasking in skeletal muscle using a novel antiserum (WU626) directed against residues 245–266 within the central cytoplasmic loop of Glut4. The immunoblot data

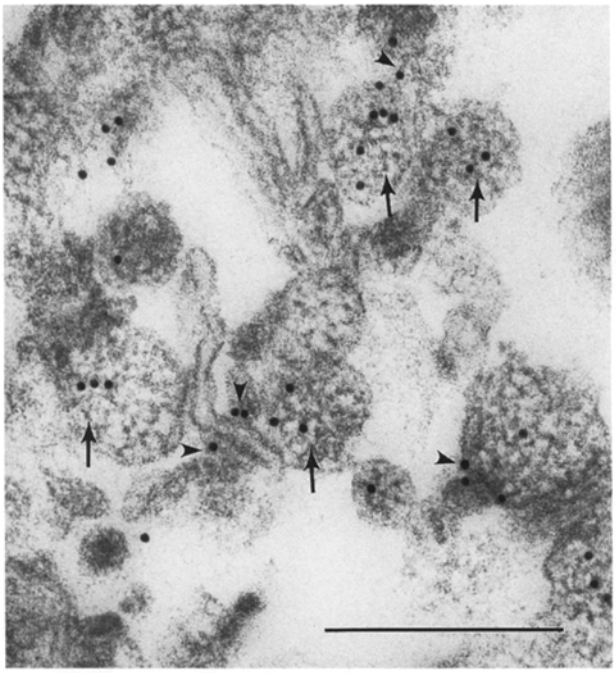

Figure 3. Ultrastructural analysis of isolated muscle triadic junctions. A subcellular fraction containing intact muscle triads was embedded in Lowricryl HM20 and stained with F349 anti-Glut4 antibody and colloidal gold secondary antibody. Both the T-tubule (*arrowhead*) and flanking terminal cisternae (*arrow*) were labeled with anti-Glut4 antibody. Bar, 0.25 μm.

shown in Fig. 5 *A* demonstrates the reactivity and specificity of the peptide affinity-purified WU626 IgG towards Glut4. This IgG was used to detect Glut4 by confocal immunofluorescence microscopy in skeletal muscle sections obtained from mice during the basal and hyperinsulinemic clamp periods. In contrast to the results obtained with the F349 antibody directed against the Glut4 COOH terminus, WU626 IgG did not provide differential labeling between the basal and hyperinsulinemic states (Fig. 4, *c* and *d*). The overall staining was weaker using the WU626 IgG than with the F349 IgG because of the much lower affinity of this antibody, which precludes its use for immunogold labeling. These data suggest that the epitope masking/unmasking is specific to the COOH terminus of Glut4.

Interestingly, insulin treatment also increased the average diameter of T-tubules (Fig. 6). The insulin-treated group exhibited an average T-tubule diameter of 60.6 ± 5.6 nm, while the basal group had an average T-tubule diameter of 40.4 ± 2.8 nm ($P < 0.005$). It is possible that this effect augments glucose transport into muscle fibers by increasing the accessibility of glucose to the narrow T-tubular channels. Additionally, this result implies that the surface area of the T-tubules has increased by ~50%, and this will increase the total Glut4 content of the T-tubules by this same percentage. Thus, the actual increase in Glut4 content of the T-tubule membrane after in vivo administration of insulin was approximately threefold rather than approximately twofold (see Table I).

The quantitative morphological data described above strongly imply that insulin-sensitive transport in muscle occurs primarily across T-tubules. To determine whether T-tubules indeed represent the structures responsible for insulin-stimulated transport, we used a glycerol shock procedure to reversibly disrupt T-tubules. This procedure has previously been used to demonstrate that T-tubules are essential for excitation–contraction coupling in skeletal muscle (15, 20, 30). Isolated rat epitrochlearis muscles were incubated in horseradish peroxidase for use as an extracellular space marker. In untreated muscle, the enzyme product was detected in the lumen of T-tubules within 30 min (Fig. 7 *A*), demonstrating the accessibility of T-tubules in normal muscle to protein-sized molecules in the extracellular fluid. After the glycerol shock treatment, enzyme product was no longer detected within T-tubules after the 30 min incubation, in agreement with previous observations (13, 41). The typical T-tubule morphology was lost, and instead many large vacuoles were observed at the spaces between myofibrils where T-tubules are normally present (Fig. 7 *B*). Immunolabeling demonstrated that these vacuoles became the predominant site of Glut4 labeling in muscle subjected to glycerol shock, suggesting that these vacuoles represent the vesiculation of T-tubule membranes (Fig. 7 *B*, *Inset*). Restoration of T-tubule morphology could be demonstrated by returning the muscle back to the glycerol-containing Ringer's buffer for 40 min, and once again enzyme product could be detected within the lumen of the T-tubules after incubation in horseradish peroxidase solution (Fig. 7 *C*).

The transport of the nonmetabolizable glucose analog, 3-*O*-methylglucose, was measured in isolated muscles either left in normal Ringer's buffer, subjected to glycerol shock, or subjected to glycerol shock and then returned to glycerol-containing Ringer's buffer in order to restore T-tubule morphology (Fig. 8). The unshocked muscles exhibited a threefold increase in transport in response to insulin. The shocked muscles exhibited a 50% increase in basal transport relative to the controls, but insulin-stimulated transport was completely abolished. Transport in muscles subjected to shock and then reversal was nearly indistinguishable from that observed in unshocked control muscles. These data are consistent with the hypothesis that insulin-stimulated transport occurs primarily across T-tubules and that most basal transport occurs across the sarcolemma.

Discussion

There is some controversy in the literature concerning the localization of glucose transporters in skeletal muscle. Friedman et al. (18) published data localizing immunogold-labeled Glut4 primarily to triadic junctions in sections of human vastus lateralis muscle embedded in LR White resin. These investigators observed little or no Glut4 on the sarcolemma either in the presence or absence of insulin. Bornemann et al. (6) used HRP-conjugated antibodies to localize Glut4 in Epon-embedded rat soleus muscle. They observed staining in vesicles beneath the sarcolemma and in terminal cisternae. Insulin administration resulted in the appearance of reaction products in the sarcolemma. Dudek et al. (12) localized surface-exposed Glut4 in rat soleus muscle by autoradiography after photolabeling with the impermeant glucose analog, 2-*N*-4-(1-azi-2,2,2-trifluoroethyl) benzoyl-1,3-bis-(D-mannose-4-yloxy)-2-propylamine (ATB-[2-^{3}H]BMPA). Their data indicate that the vast bulk of surface-exposed

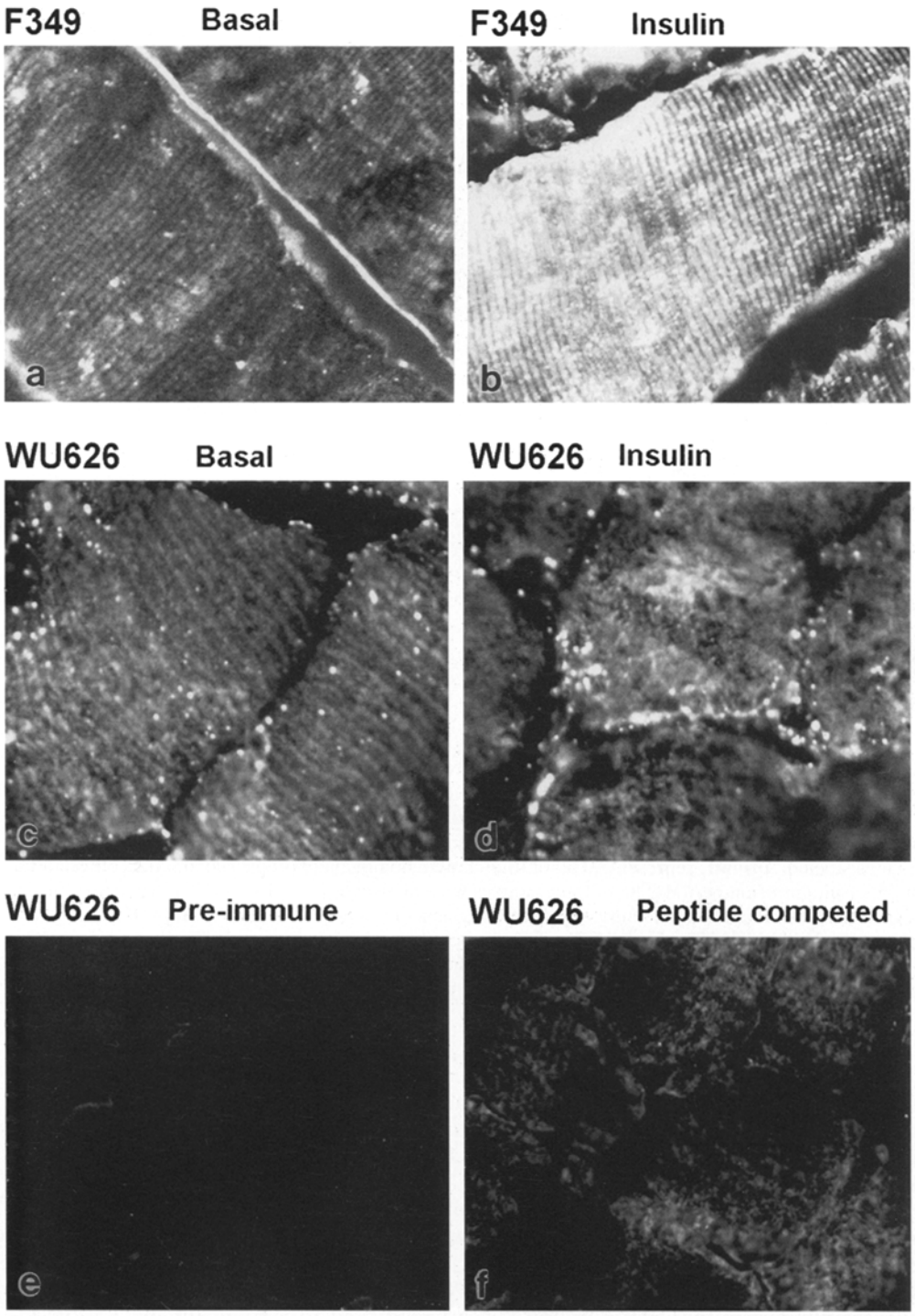

Figure 4. Laser confocal immunofluorescent staining of Glut4 in soleus/gastrocnemius/plantaris muscles of Glut4 transgenic mice using F349 and WU626 antibodies. Sections were cut and stained with F349 or WU626 anti-Glut4 primary antibody followed by fluorescein-conjugated secondary antibody. Representative fields are shown. *a* and *c* show muscle samples taken from the right hind leg at the end of the initial basal period of the hyperinsulinemic clamp study. *b*, *d*, *e*, and *f* show muscle samples taken from the left hind leg of the same mouse at the end of the insulin infusion. *a* and *b* show sections stained with 2.8 μg/ml of affinity-purified F349 IgG, *c* and *d* show sections stained with 40 μg/ml of affinity-purified WU626 IgG, *e* was stained with preimmune WU626 IgG, and *f* was stained with WU626 antibody in the presence of a 20-fold molar excess of immune peptide. The difference in staining intensity between the basal and insulin-treated muscles shown in *a* and *b* was dramatic and was reproduced in three different mice. Control fields stained with preimmune F349 IgG were black and are not shown. There was no apparent difference between staining of the basal and insulin-stimulated muscle using the WU626 antibody.

Glut4 is in T-tubules. Insulin treatment increased labeling of the exoplasmic face of the T-tubules by ~30–75%. Rodnick et al. (45) examined the subcellular distribution of Glut4 in frozen sections of rat soleus muscle by immunogold labeling. In contrast to most other studies, these investigators observed Glut4 primarily in vesicles beneath the sarcolemma close to Golgi stacks, with lesser labeling near transverse tubules. Insulin increased Glut4 only in the sarcolemma. Subcellular fractionation studies in which T-tubules were separated from the sarcolemma confirm the relative enrichment of Glut4 in T-tubules (32, 40). These studies also confirm that insulin increases the Glut4 content of both sarcolemmal and T-tubular fractions.

Our semiquantitative morphological data are in agreement with the majority of these studies, which indicate that the bulk of muscle Glut4 resides in the region of triadic junctions in the T-tubules and terminal cisternae. Assuming a muscle fiber is a cylinder with the dimensions 2 cm × 50 μm, that a sarcomere is a cylinder with the dimensions 2 μm × 1 μm, and using our measurement for the average diameter of a T-tubule after insulin stimulation of 60 nm, it can be estimated that T-tubules occupy

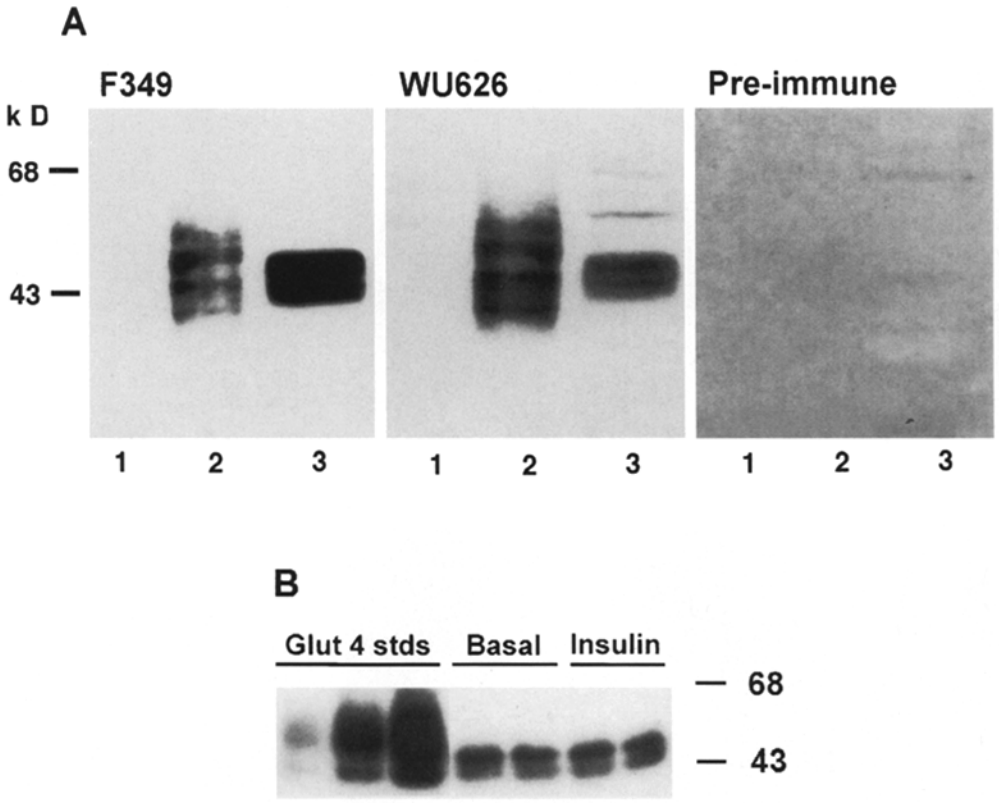

Figure 5. (*A*) Comparison of the specificity and reactivity of F349 and WU626 antibodies; (*B*) effect of short-term, high-dose insulin infusion on the Glut4 protein content of total gastrocnemius/soleus/plantaris muscle homogenates from Glut4-overexpressing transgenic mice. (*A*) Human erythrocyte membrane ghosts containing 10 ng of Glut1 (lane *1*), *Xenopus* oocyte membranes containing 10 ng of Glut4 (lane *2*), and 20 μg of total mouse skeletal muscle protein (lane *3*) were subjected to SDS-PAGE and blotted onto nitrocellulose membranes. The triplicate membranes were probed with either 0.2 μg/ml of affinity-purified F349 IgG directed against the COOH terminus of Glut4, 1 μg/ml of affinity-purified WU626 IgG directed against the central loop of Glut4, or a 1:1,500 dilution of preimmune serum from the rabbit that produced the WU626 antibody. The immunoblots were then processed as described previously (36). (*B*) The same gastrocnemius/soleus/plantaris muscle samples used for immunofluorescence analysis in Fig. 4 were split and used for Western blot analysis. The lanes labeled "Glut 4 stds" represent the equivalent of 2, 10, and 20 ng of purified Glut4 protein from oocyte membranes. The lanes labeled "Basal" represent 10 μg of total muscle homogenate from two Glut4 transgenic obtained mice at the end of the initial basal period of a hyperinsulinemic clamp study. The lanes labeled "Insulin" represent 10 μg of total muscle homogenate prepared from the contralateral limb of the same mice at the end of the insulin infusion period. The protein samples were analyzed by SDS-PAGE followed by blotting onto a nitrocellulose membrane and incubation with F349 primary antibody directed against the COOH terminus of Glut4 and ^{125}I-labeled secondary antibody. The rate of tracer-determined whole body glucose utilization was 39 mg/kg·min during the basal period and 115 mg/kg·min during the insulin infusion period. Quantification of the bands using a phosphoimager indicated that the basal and insulin muscle samples contained an average of 3.0 and 3.1 ng, respectively, of Glut4 protein per 10 μg of total muscle protein.

approximately nine times the total surface area of the sarcolemma. Since the labeling density in the presence of insulin along T-tubules was twofold greater than the labeling density along the sarcolemma, we estimate that at least 94% of Glut4-mediated uptake should occur across the T-tubule. This assumes that Glut4 is equally active in the sarcolemma and the T-tubule membrane and that glucose has equal access to both membrane surfaces. The glycerol shock experiments confirmed that most insulin-stimulated uptake occurs across the T-tubule membranes, in that osmotic disruption of the T-tubular system abolished insulin-stimulated transport in isolated muscles. The anatomical advantage of transporting sugar into muscle across T-tubules has been discussed previously (10). The T-tubular system is capable of carrying sugar deep into the muscle fiber where glycolytic enzymes are located, bypassing the diffusion barrier of the myofibrils.

We observed an insulin-stimulated increase in Glut4 immunogold reactivity in the sarcolemma and a corresponding decrease in the subsarcolemmal region, suggesting that translocation may have occurred from one compartment to the other. However, our results also suggest that the sarcolemma plays only a minor role in mediating insulin-stimulated glucose transport and that the T-tubule is the major site of insulin-stimulated transport. The threefold increase in T-tubular Glut4 after in vivo insulin administration is nearly sufficient to account for the 3.5-fold increase in whole-body glucose disposal observed for the Glut4 mice under clamp conditions, and is similar to the increase that is routinely observed for insulin-stimulated glucose transport in muscles isolated from the Glut4 transgenic mice. However, the increase in T-tubular Glut4 was not accompanied by a decrease in the intracellular Glut4 in the region of the triadic junctions. Rather, the total na-

Figure 6. Insulin administration increases the diameter of T-tubules. Electron micrographs illustrating the relative T-tubule diameter in basal (*A*) and insulin stimulated (*B*) muscles. The dilatation of the T-tubule by insulin was not uniform, but the average diameter of the T-tubules in the insulin-treated group was 50% greater than in the noninsulin-treated group. Bar, 0.5 μm.

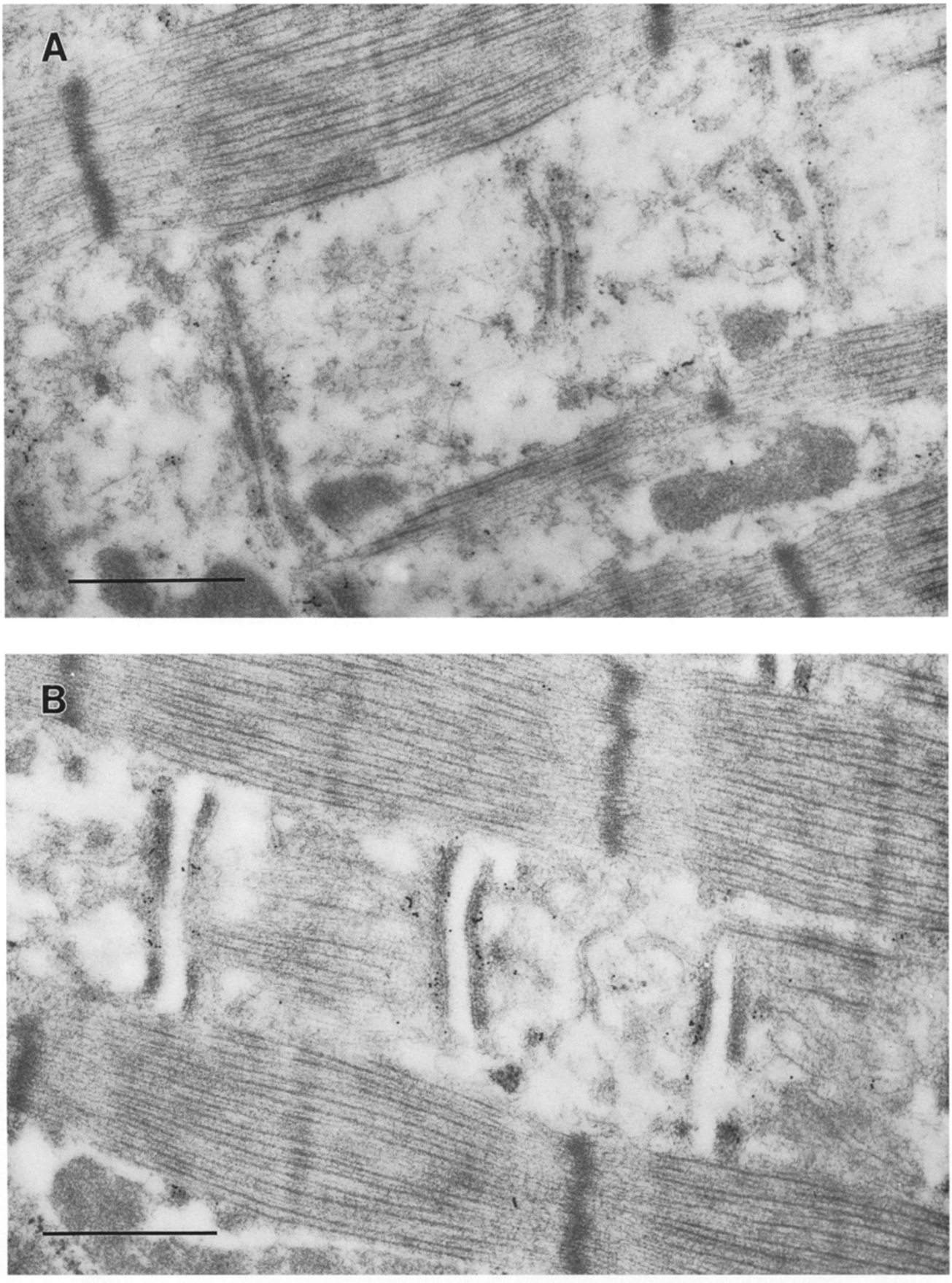
A
B

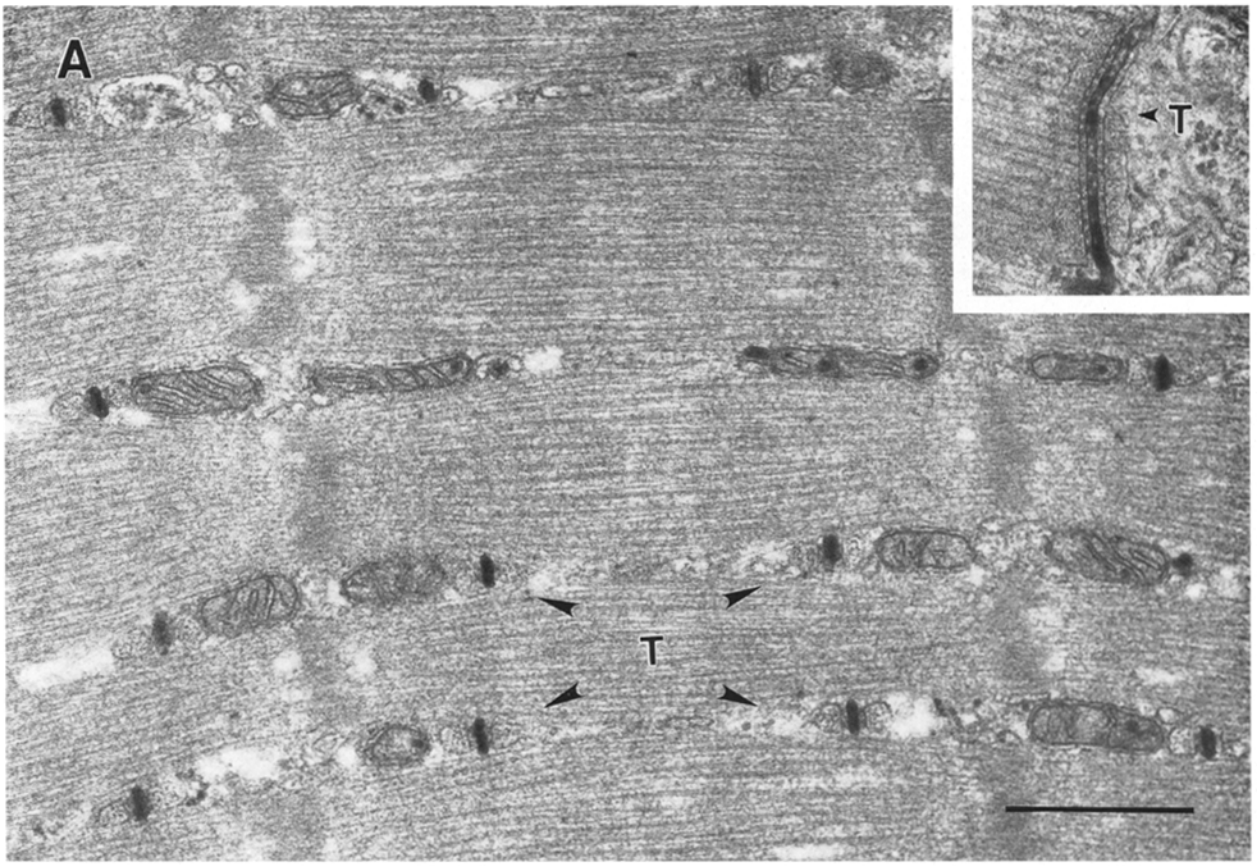
A
T
T

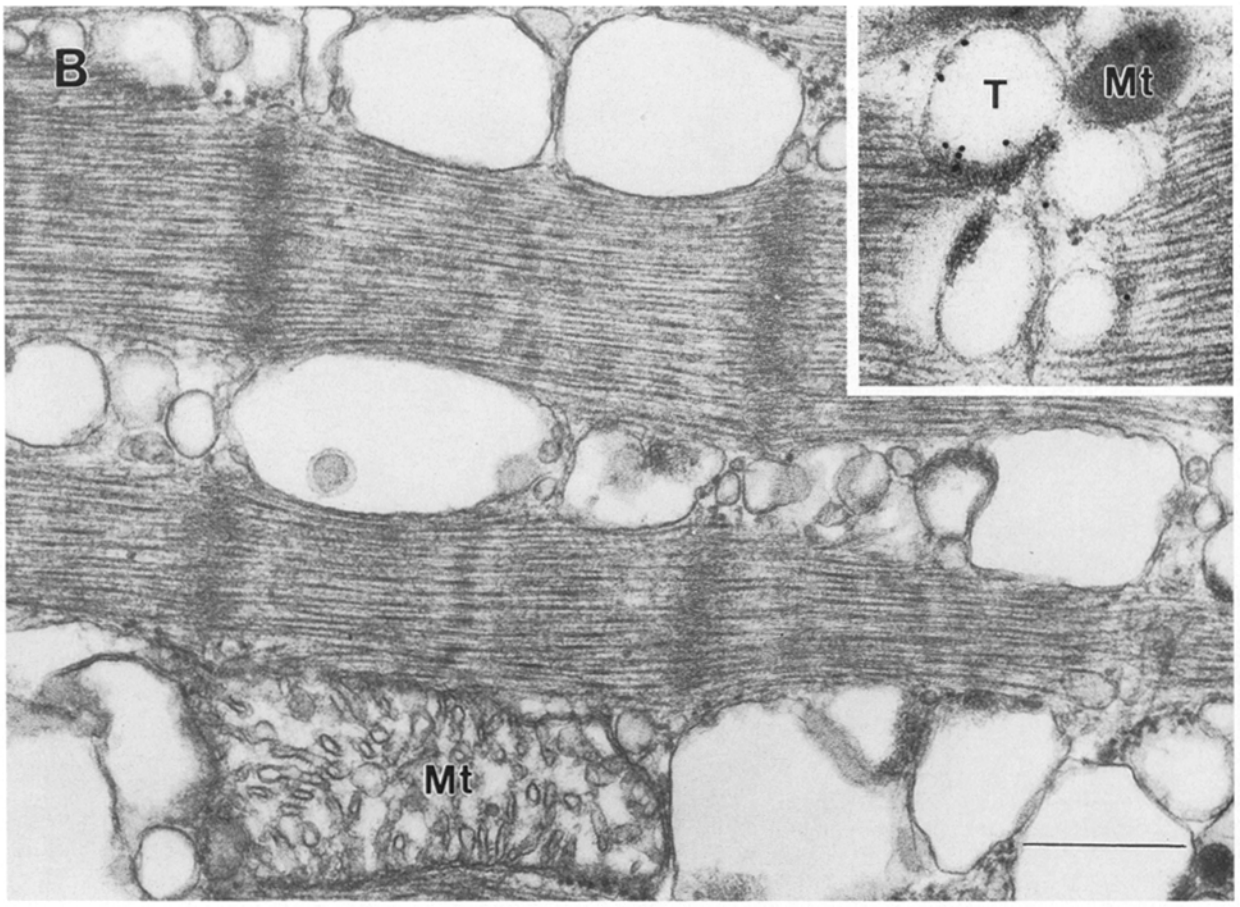
B
T
Mt
Mt

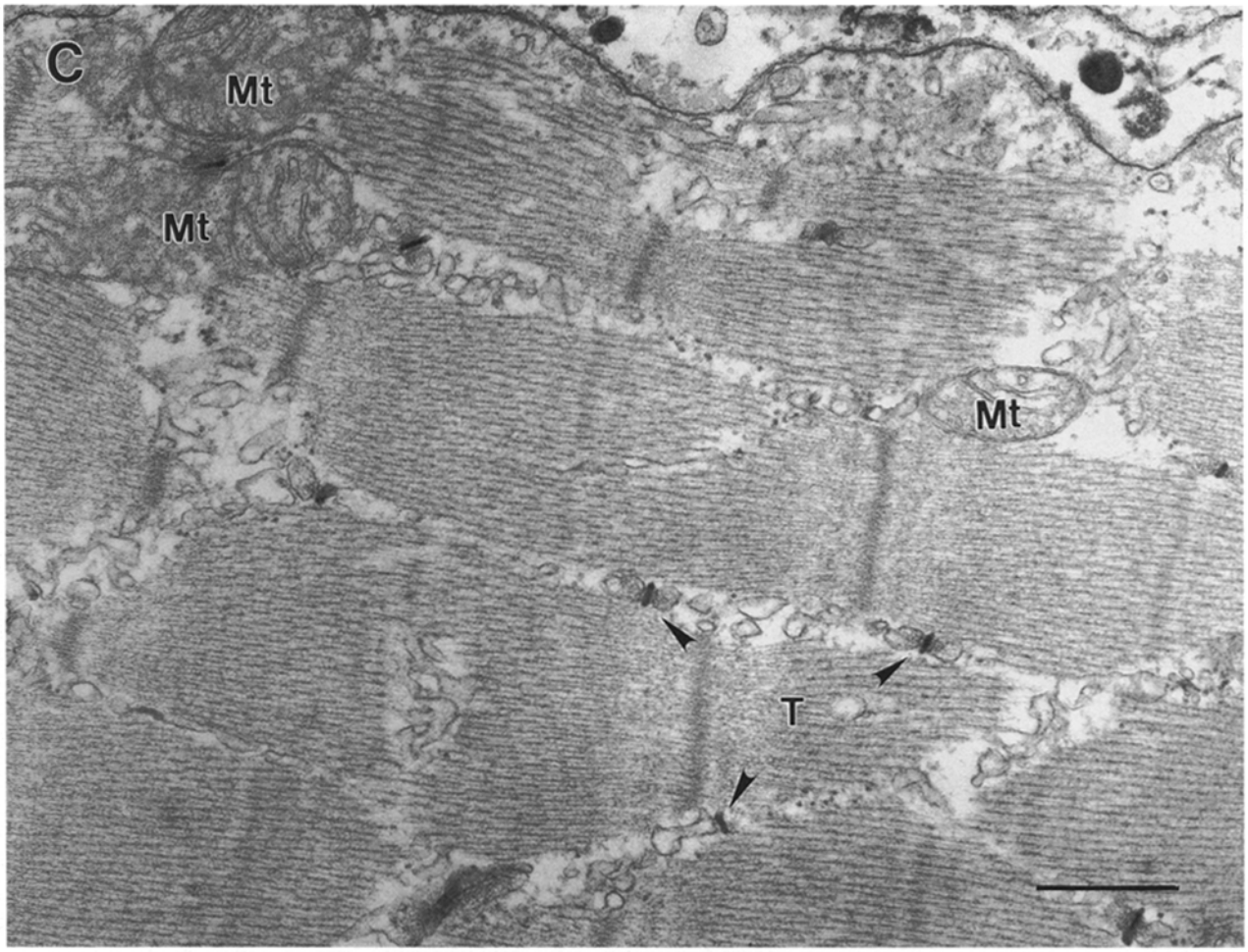

Figure 7. Disruption of T-tubules by hypertonic glycerol shock. Isolated rat epitrochlearis muscles were incubated in 2 ml of Ringer's solution in the presence or absence of 400 mM glycerol for 1 h at room temperature and then transferred to 2 ml of glycerol-free Ringer's for 30 min. To reverse the glycerol shock effect, one group of shocked muscles was returned to glycerol-containing Ringer's for 40 min. Muscles were then incubated in Ringer's buffer containing 1 mg/ml of horseradish peroxidase for 30 min. In control muscles, the electron-opaque peroxidase reaction product filled most of the T-tubule lumen (*A*), indicating that the lumen of the T-tubule is readily accessible from the extracellular fluid. In contrast, the glycerol-treated muscles developed vacuoles at the sites where T-tubules were normally located. The horseradish peroxidase product was absent from these vacuoles (*B*). The disruption of T-tubules by sequentially suspending the muscle in glycerol containing Ringer's buffer and then normal Ringer's buffer was reversible by returning the muscle to glycerol-containing Ringer's buffer as shown in (*C*). Both the typical T-tubule morphology and the accessibility to exterior tracer were recovered. The inset in *B* shows immunogold labeling with F349 anti-Glut4 antibody of the glycerol shock-induced vacuoles. *T*, T-tubule; *Mt*, mitochondria. Bar, 0.5 μm.

tive Glut4 immunoreactivity increased in frozen sections as determined by laser confocal immunofluorescence microscopy and in fixed and embedded tissue sections as assessed by immunogold electron microscopy. On the other hand, short-term insulin treatment had no effect on total skeletal muscle Glut4 protein levels as assessed by immunoblotting. Thus, these data support the hypothesis that insulin mediates a structural change in Glut4 that may precede or accompany its translocation to the T-tubule. Alternatively, it is possible that translocation to T-tubules does not occur and that the insulin-induced increase in Glut4 immunoreactivity in the T-tubule is due completely to unmasking of the COOH-terminal epitope. This same phenomenon was observed previously as an insulin-induced increase in Glut4 immunofluorescence intensity in transgenic mouse muscle. Our data indicate that the COOH-terminal epitope recognized by the antibody is more accessible in the native protein after insulin treatment.

These data are strikingly similar to those reported by Smith et al. (49), who demonstrated the unmasking of the same Glut4 COOH-terminal epitope in the adipocyte plasma membrane after insulin treatment. This region of Glut4 is of special interest because it lies in close proximity to a dileucine motif in the COOH-terminal cytoplasmic tail that confers insulin-sensitive targeting (8, 23, 51, 52). Targeting experiments conducted on chimeric glucose transporters in L6 myocytes indicate that the extreme COOH-terminus of Glut4 downstream of the dileucine is also important for this targeting behavior (23). Thus, we hypothesize that in the basal state, the COOH terminus of native Glut4 is partially inaccessible to antibody due to its specific conformational state or to its interaction with an-

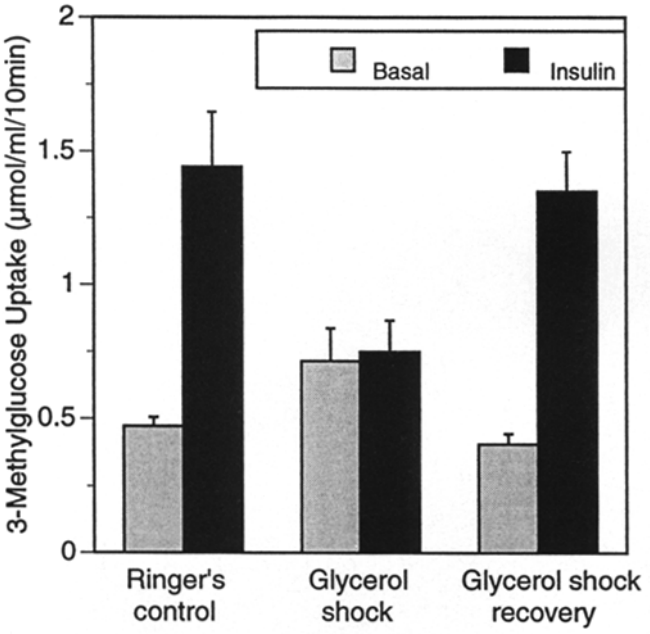

Figure 8. Disruption of T-tubules abolishes insulin-stimulated glucose transport. Isolated rat epitrochlearis muscles were incubated in 2 ml of Ringer's solution in the presence or absence of 400 mM glycerol for 1 h at room temperature and then transferred to 2 ml glycerol-free Ringer's for 30 min. To reverse the glycerol shock effect, one group of shocked muscles was returned to glycerol-containing Ringer's for 40 min. The muscles were then incubated for 20 min at 35°C in 2 ml of oxygenated Krebs-Henseleit buffer supplemented with 2 mM sodium pyruvate, 36 mM mannitol, and 0.1% BSA, in the presence or absence of 10 mU/ml insulin, before measurement of glucose transport activity. A control group was also included to demonstrate that direct incubation in 400 mM glycerol did not affect glucose transport (not shown). The results shown are the average of measurements conducted using eight animals per group. The error bar represents the standard error. The insulin-stimulated transport values for the control and glycerol-shocked groups are significantly different ($P < 0.05$).

other protein. Insulin may act to either alter the conformation of the COOH terminus or to disrupt the protein–protein interaction and thus increase the accessibility of the epitope. One obvious possibility is that a specific targeting factor interacts with the COOH terminus of Glut4 in the basal state, and that this interaction is involved in maintaining the intracellular distribution of the molecule.

Most of the skeletal muscle Glut4 was localized at the triadic junction in T-tubules and in what appeared to be terminal cisternae of the sarcoplasmic reticulum. The sarcoplasmic reticulum is generally considered to be the equivalent of the endoplasmic reticulum in other types of cells. It is thus not obvious why these structures should possess high concentrations of glucose transporters, whose sole function is to transport glucose from the extracellular fluid into the muscle cytoplasm. There are at least three possible explanations for this observation: (1) Glut4 in the terminal cisternae may represent an intracellular reserve pool from which translocation occurs; (2) as some authors have suggested (18), the Glut4 in this region may actually be present in distinct vesicles from which translocation occurs and that cannot be distinguished from the terminal cisternae by the techniques used; or (3) they may represent a pathway by which glucose is able to freely diffuse across the T-tubules, into the sarcoplasmic reticulum, and then into the cytosol. The T-tubules are surrounded by membranes of the terminal cisternae. There is a 10–13-nm space between the T-tubule membrane and the terminal cisternae, but at intervals, terminal cisternae form periodic pillars that connect the two apposed membranes (14). This contact has been postulated to be the structural basis for the transmission of the depolarization current to the interior sarcoplasmic reticulum system. The currently accepted view is that T-tubules are permanently open to the extracellular space but that the sarcoplasmic reticulum is not in a permanently open connection with either the T-tubule or the extracellular space. Nevertheless, there are observations suggesting that the sarcoplasmic reticulum is accessible from the extracellular space. For example, the sarcoplasmic reticulum may change its volume in relation to changes in the osmotic pressure in the bath solution (2), and extracellular peroxidase may have access to the sarcoplasmic reticulum under certain conditions (47). Glut4 in the terminal cisternae and the sarcoplasmic reticulum may thus provide a necessary pathway by which glucose diffuses from the lumen of the T-tubules into the cytosol.

Glut1 was localized primarily to the sarcolemma in the muscle of Glut1 transgenic mice, and, unlike Glut4, its distribution and abundance did not change in response to insulin. This is consistent with the observation that the muscle of Glut1 transgenic mice exhibit up to a sevenfold increase in basal glucose transport compared to nontransgenic littermates (44). Although it is possible that some mistargeting of Glut1 occurred in the transgenic muscle because of the level of overexpression, there is no reason to suspect that the general distribution of Glut1 in normal muscle is different from that observed in the transgenic muscle. Our data are in agreement with the subcellular fractionation studies of Marette et al. (33) conducted on the muscle of normal rats, as well as Glut1 localization studies conducted on cultured L6 myocytes (23) and BC3H-1 myocytes (16). Taken together, these data strongly argue that Glut1 resides constitutively in the sarcolemma and provides muscle fibers with the low level of glucose they require in the basal, resting state. Glut1 is thus targeted differently in skeletal muscle than in adipocytes, where it is enriched in intracellular compartments in the basal state and translocates to the plasma membrane in response to insulin (55). It is of considerable interest that Glut1 and Glut4 are targeted to distinct plasma membrane domains in skeletal muscle, because very little is currently known about protein trafficking in skeletal muscle and how the distinct composition of the muscle membrane systems arises. The glucose transporters provide an excellent model system to study the sorting of proteins to distinct plasma membrane domains in skeletal muscle.

Morphological analysis of T-tubules in basal and insulin-treated muscle demonstrated that insulin increased the average diameter of the tubules in longitudinal sections. The observed increase is consistent with an increase in total T-tubule surface area from 5.8- to 8.6-fold of the total sarcolemmal surface area of a hypothetical muscle fiber 2 cm × 50 μm. This may represent a mechanism by which

insulin enhances the ability of glucose to permeate muscle tissue by increasing the rate of diffusion of glucose into the narrow membranous channels. Insulin is also known to enhance capillary blood flow in skeletal muscle (1). Thus, this hormone appears to act at multiple sites to facilitate the uptake of glucose into skeletal muscle.

Supported in part by National Institutes of Health grants DK38495, DK50332 (M. Mueckler), and DK18986 (J.O. Holloszy) and by the Diabetes Research and Training Center at Washington University Medical School. W. Wang was supported by a mentor-based postdoctoral fellowship from the American Diabetes Association. B.A. Marshall was supported by the John Henry and Bernadine Foster Foundation and is a Scholar of the Child Health Research Center of Excellence in Developmental Biology at Washington University School of Medicine (HD 33688).

Received for publication 10 April 1996 and in revised form 21 June 1996.

References

1. Baron, A.D., H. Steinberg, G. Brechtel, and A. Johnson. 1994. Skeletal muscle blood flow independently modulates insulin-mediated glucose uptake. *Am. J. Physiol.* 266:E248–E253.
2. Birks, R.I., and D.F. Davey. 1969. Osmotic responses demonstrating the extracellular character of the sarcoplasmic reticulum. *J. Physiol.* 202: 171–188.
3. Birnbaum, M.J. 1989. Identification of a novel gene encoding an insulin-responsive glucose transporter protein. *Cell.* 57:305–315.
4. Birnbaum, M.J., H.C. Haspel, and O.M. Rosen. 1986. Cloning and characterization of a cDNA encoding the rat brain glucose-transporter protein. *Proc. Natl. Acad. Sci. USA.* 83:5784–5788.
5. Bonadonna, R.C., P.S. Del, M.P. Saccomani, E. Bonora, G. Gulli, E. Ferrannini, D. Bier, C. Cobelli, and R.A. DeFronzo. 1993. Transmembrane glucose transport in skeletal muscle of patients with non-insulin-dependent diabetes. *J. Clin. Invest.* 92:486–494.
6. Bornemann, A., T. Ploug, and H. Schmalbruch. 1992. Subcellular localization of GLUT4 in nonstimulated and insulin-stimulated soleus muscle of rat. *Diabetes.* 41:215–221.
7. Charron, M.J., F.D. Brosius, S.L. Alper, and H.F. Lodish. 1989. A glucose transport protein expressed predominately in insulin-responsive tissues. *Proc. Natl. Acad. Sci. USA.* 86:2535–2539.
8. Corvera, S., A. Chawla, R. Chakrabarti, M. Joly, J. Buxton, and M.P. Czech. 1994. A double leucine within the GLUT4 glucose transporter COOH-terminal domain functions as an endocytosis signal. (Published erratum appears in *J. Cell Biol.* 1994. 126:1625.) *J. Cell Biol.* 126:979–989.
9. Cushman, S.W., and L.J. Wardzala. 1980. Potential mechanism of insulin action on glucose transport in the isolated rat adipose cell. Apparent translocation of intracellular transport systems to the plasma membrane. *J. Biol. Chem.* 255:4758–4762.
10. Dohm, G.L., P.L. Dolan, W.R. Frisell, and R.W. Dudek. 1993. Role of transverse tubules in insulin stimulated muscle glucose transport. *J. Cell Biochem.* 52:1–7.
11. Douen, A.G., E. Burdett, T. Ramlal, S. Rastogi, M. Vranic, and A. Klip. 1991. Characterization of glucose transporter-enriched membranes from rat skeletal muscle: assessment of endothelial cell contamination and presence of sarcoplasmic reticulum and transverse tubules. *Endocrinology.* 128:611–616.
12. Dudek, R.W., G.L. Dohm, G.D. Holman, S.W. Cushman, and C.M. Wilson. 1994. Glucose transporter localization in rat skeletal muscle. Autoradiographic study using ATB-[2-^{3}H]BMPA photolabel. *FEBS Lett.* 339: 205–208.
13. Eisenberg, B., and R.S. Eisenberg. 1968. Selective disruption of the sarcotubular system in frog sartorius muscle. *J. Cell Biol.* 39:451–467.
14. Eisenberg, B.R., and R.S. Eisenberg. 1982. The T-SR junction in contracting single skeletal muscle fibers. *J. Gen. Physiol.* 79:1–19.
15. Eisenberg, R.S., J.N. Howell, and P.C. Vaughan. 1971. The maintenance of resting potentials in glycerol-treated muscle fibres. *J. Physiol.* 215:95–102.
16. El-Kebbi, I.M., S. Roser, R.J. Pollet, S.W. Cushman, and C.M. Wilson. 1994. Regulation of the GLUT1 glucose transporter in cultured myocytes: total number and subcellular distribution as determined by photoaffinity labeling. *Biochem. J.* 301:35–40.
17. Ferrannini, E., O. Bjorkman, G.A. Reichard, A. Pilo, M. Olsson, J. Wahren, and R.A. DeFronzo. 1985. The disposal of an oral glucose load in healthy subjects. *Diabetes.* 34:580–588.
18. Friedman, J.E., R.W. Dudek, D.S. Whitehead, D.L. Downes, W.R. Frisell, J.F. Caro, and G.L. Dohm. 1991. Immunolocalization of glucose transporter GLUT4 within human skeletal muscle. *Diabetes.* 40:150–154.
19. Fukumoto, H., T. Kayano, J.B. Buse, Y. Edwards, P.F. Pilch, G.I. Bell, and S. Seino. 1989. Cloning and characterization of the major insulin-responsive glucose transporter expressed in human skeletal muscle and other insulin-responsive tissues. *J. Biol. Chem.* 264:7776–7779.
20. Gate, P.W., and R.S. Eisenberg. 1967. Action potentials without contraction in frog skeletal muscle fibers with disrupted transverse tubules. *Science (Wash. DC).* 158:1702–1703.
21. Gulve, E.A., J.M. Ren, B.A. Marshall, J. Gao, P.A. Hansen, J.O. Holloszy, and M. Mueckler. 1994. Glucose transport activity in skeletal muscles from transgenic mice overexpressing GLUT1. Increased basal transport is associated with a defective response to diverse stimuli that activate GLUT4. *J. Biol. Chem.* 269:18366–18370.
22. Haney, P.M., J.W. Slot, R.C. Piper, D.E. James, and M. Mueckler. 1991. Intracellular targeting of the insulin-regulatable glucose transporter (GLUT4) is isoform specific and independent of cell type. *J. Cell Biol.* 114:689–699.
23. Haney, P.M., M.A. Levy, M.S. Strube, and M. Mueckler. 1995. Insulin-sensitive targeting of the GLUT4 glucose transporter in L6 myoblasts is conferred by its COOH-terminal cytoplasmic tail. *J. Cell Biol.* 129:641–658.
24. Hansen, P.A., E.A. Gulve, B.A. Marshall, J. Gao, J.E. Pessin, J.O. Holloszy, and M. Mueckler. 1995. Skeletal muscle glucose transport and metabolism are enhanced in transgenic mice overexpressing the Glut4 glucose transporter. *J. Biol. Chem.* 270:1679–1684.
25. Hirshman, M.F., L.J. Goodyear, L.J. Wardzala, E.D. Horton, and E.S. Horton. 1990. Identification of an intracellular pool of glucose transporters from basal and insulin-stimulated rat skeletal muscle. *J. Biol. Chem.* 265: 987–991.
26. Holman, G.D., I.J. Kozka, A.E. Clark, C.J. Flower, J. Saltis, A.D. Habberfield, I.A. Simpson, and S.W. Cushman. 1990. Cell surface labeling of glucose transporter isoform GLUT4 by bis-mannose photolabel. Correlation with stimulation of glucose transport in rat adipose cells by insulin and phorbol ester. *J. Biol. Chem.* 265:18172–18179.
27. Hresko, R.C., M. Kruse, M. Strube, and M. Mueckler. 1994. Topology of the Glut 1 glucose transporter deduced from glycosylation scanning mutagenesis. *J. Biol. Chem.* 269:20482–20488.
28. Hresko, R.C., H. Murata, B.A. Marshall, and M. Mueckler. 1994. Discrete structural domains determine differential endoplasmic reticulum to Golgi transit times for glucose transporter isoforms. *J. Biol. Chem.* 269: 32110–32119.
29. James, D.E., M. Strube, and M. Mueckler. 1989. Molecular cloning and characterization of an insulin regulatable glucose transporter. *Nature (Lond.).* 338:83–87.
30. Krolenko, S.A. 1969. Changes in the T-system of muscle fibres under the influence of influx and efflux of glycerol. *Nature (Lond.).* 221:966–968.
31. Liu, M.-L., E.M. Gibbs, S.C. McCoid, A.J. Milici, H.A. Stukenbrok, R.K. McPherson, J.L. Treadway, and J.E. Pessin. 1993. Transgenic mice expressing the human GLUT4/muscle-fat facilitative glucose transporter protein exhibit efficient glycemic control. *Proc. Natl. Acad. Sci. USA.* 90: 11346–11350.
32. Marette, A., E. Burdett, A. Douen, M. Vranic, and A. Klip. 1992. Insulin induces the translocation of GLUT4 from a unique intracellular organelle to transverse tubules in rat skeletal muscle. *Diabetes.* 41:1562–1569.
33. Marette, A., J.M. Richardson, T. Ramlal, T.W. Balon, M. Vranic, J.E. Pessin, and A. Klip. 1992. Abundance, localization, and insulin-induced translocation of glucose transporters in red and white muscle. *Am. J. Physiol.* 263:C443–C452.
34. Marshall, B.A., and M.M. Mueckler. 1994. Differential effects of GLUT-1 or GLUT-4 overexpression on insulin responsiveness in transgenic mice. *Am. J. Physiol.* 267:E738-E744.
35. Marshall, B.A., H. Murata, R.C. Hresko, and M. Mueckler. 1993. Domains that confer intracellular sequestration of the Glut4 glucose transporter in Xenopus oocytes. *J. Biol. Chem.* 268:26193–26199.
36. Marshall, B.A., J.M. Ren, D.W. Johnson, E.M. Gibbs, J.S. Lillquist, W.C. Soeller, J.O. Holloszy, and M. Mueckler. 1993. Germline manipulation of glucose homeostasis via alteration of glucose transporter levels in skeletal muscle. *J. Biol. Chem.* 268:18442–18445.
37. Mitchell, R.D., P. Palade, and S. Fleischer. 1983. Purification of morphologically intact triad structures from skeletal muscle. *J. Cell Biol.* 96:1008–1016.
38. Mueckler, M. 1995. Glucose transport and glucose homeostasis: new insights from transgenic mice. *News Physiol. Sci.* 10:22–29.
39. Mueckler, M., C. Caruso, S.A. Baldwin, M. Panico, I. Blench, H.R. Morris, W.J. Allard, G.E. Lienhard, and H.F. Lodish. 1985. Sequence and structure of a human glucose transporter. *Science (Wash. DC).* 229:941–945.
40. Munoz, P., M. Rosemblatt, X. Testar, M. Palacin, G. Thoidis, P.F. Pilch, and A. Zorzano. 1996. The T-tubule is a cell-surface target for insulin-regulated recycling of membrane proteins in skeletal muscle. *Biochem. J.* 312:393–400.
41. Nakajima, S., Y. Nakajima, and L.D. Peachey. 1973. Speed of repolarization and morphology of glycerol-treated frog muscle fibres. *J. Physiol.* 234:465–480.
42. Olson, A.L., M.L. Liu, R.W.S. Moye, J.B. Buse, G.I. Bell, and J.E. Pessin. 1993. Hormonal/metabolic regulation of the human GLUT4/muscle-fat facilitative glucose transporter gene in transgenic mice. *J. Biol. Chem.* 268:9839–9846.
43. Parekh, B.S., P.W. Schwimmbeck, and M.J. Buchmeier. 1989. High effi-

ciency immuno-affinity purification of anti-peptide antibodies on thiopropyl Sepharose immunoadsorbants. *Pept. Res.* 2:249–252.
44. Ren, J.M., B.A. Marshall, E.A. Gulve, J. Gao, D.W. Johnson, J.O. Holloszy, and M. Mueckler. 1993. Evidence from transgenic mice that glucose transport is rate-limiting for glycogen deposition and glycolysis in skeletal muscle. *J. Biol. Chem.* 268:16113–16115.
45. Rodnick, K.J., J.W. Slot, D.R. Studelska, D.E. Hanpeter, L.J. Robinson, H.J. Geuze, and D.E. James. 1992. Immunocytochemical and biochemical studies of GLUT4 in rat skeletal muscle. *J. Biol. Chem.* 267:6278–6285.
46. Rothman, D.L., R.G. Shulman, and G.I. Shulman. 1992. ^{31}P nuclear magnetic resonance measurements of muscle glucose-6-phosphate. Evidence for reduced insulin-dependent muscle glucose transport or phosphorylation activity in non-insulin-dependent diabetes mellitus. *J. Clin. Invest.* 89:1069–1075.
47. Rubio, R., and N. Sperelakis. 1972. Penetration of horseradish peroxidase into the terminal cisternae of frog skeletal muscle. *Z. F. Zellforsc. Mikrosk. Anat.* 124:57–71.
48. Slot, J.W., H.J. Geuze, S. Gigengack, G.E. Lienhard, and D.E. James. 1991. Immuno-localization of the insulin regulatable glucose transporter in brown adipose tissue of the rat. *J. Cell Biol.* 113:123–135.
49. Smith, R.M., M.J. Charron, N. Shah, H.F. Lodish, and L. Jarett. 1991. Immunoelectron microscopic demonstration of insulin-stimulated translocation of glucose transporters to the plasma membrane of isolated rat adipocytes and masking of the carboxyl-terminal epitope of intracellular GLUT4. *Proc. Natl. Acad. Sci. USA.* 88:6893–6897.
50. Treadway, J.L., D.M. Hargrove, N.A. Nardone, R.K. McPherson, J.F. Russo, A.J. Milici, H.A. Stukenbrok, E.M. Gibbs, R.W. Stevenson, and J.E. Pessin. 1994. Enhanced peripheral glucose utilization in transgenic mice expressing the human GLUT4 gene. *J. Biol. Chem.* 269:29956–29961.
51. Verhey, K.J., and M.J. Birnbaum. 1994. A Leu-Leu sequence is essential for COOH-terminal targeting signal of GLUT4 glucose transporter in fibroblasts. *J. Biol. Chem.* 269:2353–2356.
52. Verhey, K.J., J.I. Yeh, and M.J. Birnbaum. 1995. Distinct signals in the GLUT4 glucose transporter for internalization and for targeting to an insulin-responsive compartment. *J. Cell Biol.* 130:1071–1079.
53. Wilson, C.M., and S.W. Cushman. 1994. Insulin stimulation of glucose transport activity in rat skeletal muscle: increase in cell surface GLUT4 as assessed by photolabeling. *Biochem. J.* 299:755–759.
54. Young, D.A., H.J. Uhl, G.D. Cartee, and J.O. Holloszy. 1986. Activation of glucose transport in muscle by prolonged exposure to insulin. *J. Biol. Chem.* 261:16049–16053.
55. Zorzano, A., W. Wilkinson, N. Kotliar, G. Thoidis, B.E. Wadzinkski, A.E. Ruoho, and P.F. Pilch. 1989. Insulin-regulated glucose uptake in rat adipocytes is mediated by two transporter isoforms present in at least two vesicle populations. *J. Biol. Chem.* 264:12358–12363.